Energy performance optimization of combined Brayton and two parallel inverse Brayton cycles with regeneration before the inverse cycles

Z. Zhang, L. Chen *, **F. Sun**

College of Naval Architecture and Power, Naval University of Engineering, Wuhan 430033, China

Abstract This paper proposes combined regenerative Brayton and two parallel inverse Brayton cycles with regeneration before the inverse cycles. Performance analysis and optimization for the combined cycle are performed based on the first law. The analytical formulae of thermal efficiency and specific work are derived. The performance analysis and optimization of thermal efficiency and specific work are carried out by adjusting the compressor pressure ratios of the bottom cycles. The influences of the effectiveness of the regenerator and other parameters on the optimal thermal efficiency and the optimal specific work are analyzed by numerical examples. It is found that the combined regenerative cycle can obtain higher thermal efficiency than that of the base cycle but with smaller specific work. It is revealed that if the effectiveness of regenerator equals to 0.9, the combined cycles will attain an optimal thermal efficiency of 51.2%.

1. Introduction

Nowadays, gas turbines are widely used as power and energy plants. In order to meet the growing demands of energy-saving and environmental protection, an increasing number of proposals on new configurations of the gas turbine cycle (i.e. Brayton cycle) is seen, which could potentially obtain a better performance and release less pollution.

Frutschi and Plancherel [1] studied two basic gas turbine plants with water injection. In steam injection gas turbine (STIG), the steam is raised in a heat recovery steam generator downstream of the turbine, and is injected into the combustion chamber or into the turbine nozzle guide vanes. The evaporative gas turbine (EGT) in which water is injected into the compressor outlet and is evaporated there, and then the mixture will be further heated in the cold-side of the heat exchanger. It enters the combustion chamber and then passes through the turbine and the hot-side of the heat exchanger. It was found that STIG cycle shows substantial improvement on the simple Brayton cycle, mainly in specific work and also in thermal efficiency; and EGT cycle increases the thermal efficiency while the optimum pressure ratio is still quite low.

Vecchiarelli et al. [2] proposed a modified Brayton cycle in which the usual constant pressure heat addition would be constrained to a given temperature and then further heat addition is carried out in a manner approaching an isothermal process. It was found that the emissions of NO_x may be reduced by as much as 50% owing to the limited peak combustion temperature of the overall heat addition process, thus offering an environmental benefit. Moreover, the modified Brayton cycle has significant efficiency improvement of over 4% compared with conventional Brayton engines.

Horlock [3] studied the Brayton cycle with turbine cooling. In the earlier researches, it has been emphasized that the thermal efficiency of the gas turbine increases with its maximum temperature. However, in practice, higher maximum temperature requires improved combustion technology, particularly if an increase in harmful emissions such as NO_x is to be avoided. Without improvement in materials or heat transfer, it is doubtful whether much higher maximum temperature can be achieved

* Corresponding author. Tel.: +86 27 83615046; fax: +86 27 83638709.
  E-mail addresses: lgchenna@yahoo.com, lingenchen@hotmail.com
(L. Chen).
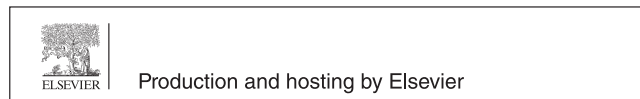
Nomenclature

c	Specific heat (kJ/(kgK))
h	Enthalpy (kJ/kg)
k	Ratio of the specific heats
P	Pressure (kPa)
q	Heat (kJ/kg)
T	Temperature (K)
w	Specific work output (kJ/kg)

Greek symbols

ε	Effectiveness of the regenerator/the heat exchanger
φ	Pressure ratio
η	Thermal efficiency
τ	Temperature ratio

Subscripts

b	Burner
c	Compressor
in	Input
max	Maximum
opt	Optimal
p	Pressure
R	Regenerator
t	Turbine
1–12	State points/sequence number

Figure 1: System layout of the combined regenerative Brayton and two parallel inverse Brayton cycles.

Figure 2: T–s diagrams for the combined regenerative Brayton and two parallel inverse Brayton cycles.

in practice; as a result, a practical limit on plant efficiency may be near, before the stoichiometric limit is reached.

The exhaust gases contain a lot of waste heat content, so using regenerator to recover a part of waste heat energy has been widely applied to improve the energy consumption of gas turbine cycles. Sato [4] studied the performance of conventional regenerated gas turbine cycles. It was found that the gas turbine cycle with regenerator can augment thermal efficiency with little effect on the work output. Second, waste heat of the exhaust gases also can be further used as heat reservoir for steam or other power plants through using heat exchanger. Combined steam and gas cycles are widely used in mid and large scale power productions due to their high efficiency and reliability [5]. The waste heat of the gas turbine is used as heat reservoir for the steam power plant in these combined cycles. These cycle types are considered the most effective power plants and thermal efficiency of these cycle types exceeded 55% several years ago and is now at approximately 60%.

Thermal efficiency and power of gas turbines can also be improved by expanding the exhaust gases further below the atmosphere condition, so various cycles are used as bottom cycles combined with simple Brayton cycle to extend the expansion process of turbines [6–9]. Frost et al. [6] proposed a hybrid gas turbine cycle (Brayton/Ericsson) as "an alternative to conventional combined gas and steam turbine power plant" which was termed as Braysson cycle. Agnew et al. [9] proposed a combined Brayton and inverse Brayton cycle. The top cycle (Brayton cycle) is used as a gas generator to power the bottom cycles (inverse Brayton cycle), and the bottom cycle produces the power output. The performance of the combined cycle was analyzed by using the commercial process simulation package. It reveals that the performance of this combined
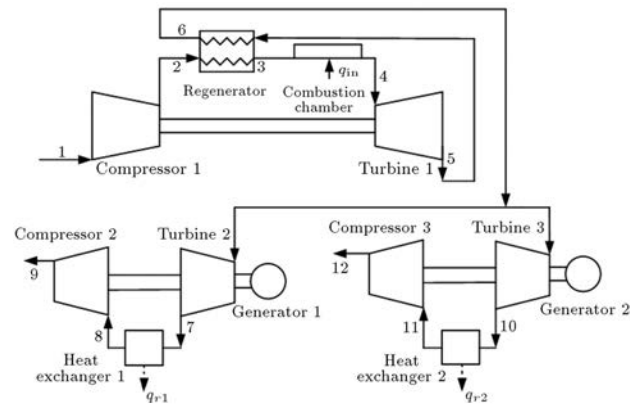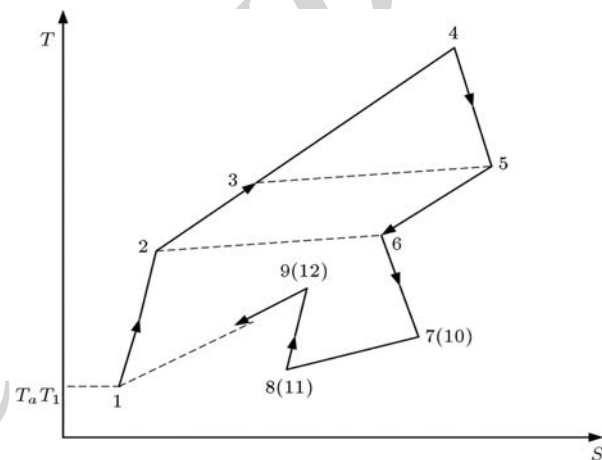
cycle is superior to simple gas turbine cycle. Based on the combined Brayton and inverse Brayton cycles, Alabdoadaim et al. [10] proposed its developed configurations including regenerative cycle and reheat cycle, and found that the system with regenerator could attain higher thermal efficiency than the base system but smaller work output based on the first law analysis. Alabdoadaim et al. [11,12] also proposed combined Ranking, Brayton and (two parallel) inverse Brayton cycles. The combined Brayton and two parallel Brayton cycles [11] can be realized by splitting the Brayton cycle exhaust gases into two equal flows and incorporating two inverse Brayton cycles with a Rankine cycle linked by heat exchangers to generate steam for a steam turbine. The use of two inverse Brayton cycles provides an opportunity for the steam to be heated in two locations, heat exchanger 1 and heat exchanger 2, which can be considered to be an evaporator and a superheater, respectively. Fujii et al. [7] also demonstrated that the choice of two parallel bottoming cycles were better than a single cycle in terms of component size, mechanical stress and manufacturing difficulties.

For combined steam and gas turbine cycles, the use of two inverse parallel inverse Brayton cycles provides an opportunity for the steam to be heated in the two heat exchangers which can be considered as an evaporator and a super heater, respectively. All of these works mentioned above [6–12] were performed based on the fist law of thermodynamics.
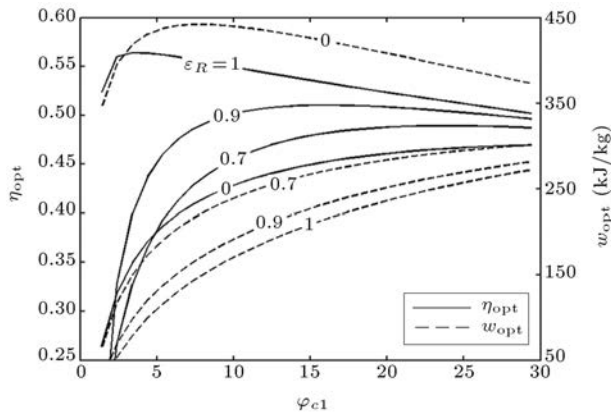
Figure 3: Influence of ε_R on the η_{opt}–φ_{c1} and w_{opt}–φ_{c1} characteristics.
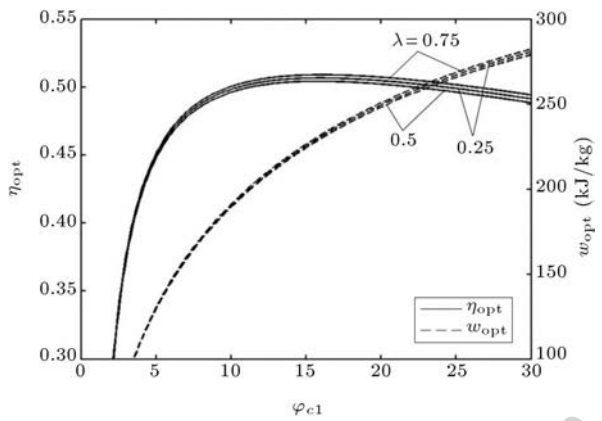

Figure 4: Influence of λ on the η_{opt}–φ_{c1} and w_{opt}–φ_{c1} characteristics.

The exergy analysis and optimization of the Braysson cycle [6] showed that the exergy loss of the combustion was the largest in the Braysson cycle, and both specific work and exergy efficiency of the cycle were larger than those of Brayton cycle [13]. The exergy analysis and optimization of the combined Brayton and inverse Brayton cycles [9] were

performed by Zhang et al. [14]. It was shown that the exergy loss of combustion chamber was the largest in the combined cycle and followed by heat exchanger. The combined cycle should be combined with Rankine cycle in order to increase the exergy efficiency. Moreover, Zhang et al. [15] performed the exergy analysis and optimization of the Brayton and two parallel inverse Brayton cycles [11]. All of these works mentioned above [13–15] were performed based on the second law of thermodynamics.

Furthermore, the power, power density and efficiency optimizations were performed for the Braysson cycle [6] by Chen et al. [16,17]. It was found that two pairs of optimum distribution of heat conductance and optimum working fluid temperature ratio existed, which led to the double maximum dimensionless power output, and double maximum dimensionless power density, respectively. Zhang et al. [18–20] also performed the power and efficiency optimizations for the combined Brayton and inverse Brayton cycles [9] as well as the Brayton and two parallel inverse Brayton cycles [11], respectively. It was found that the net power output has a maximum with respect to the air mass flow rate. It was also found that if the total size of the combined cycle power plant is taken as a constraint, there exists another optimal compressor pressure ratio of the top cycle corresponding to the maximum efficiency. All of these works mentioned above [16–20] were performed based on the finite time thermodynamics [21–33] for gas turbine cycles. The principle of optimally tuning the air flow rate and subsequent distribution of pressure drops has been used.

In addition to the cycle models proposed in [6–12], there is no new cycle configuration in the open literature. Based on the cycle models proposed in [10,11], this paper proposes a new configuration of combined regenerative Brayton and two parallel inverse Brayton cycles with regeneration before the inverse cycles. The purpose of this combined cycle is to improve the utilization of heat energy by using a regenerator to recover a part of heat energy before working fluid entering the turbine of the inverse Brayton cycle, and expanding the exhaust gases further below the atmosphere condition by using two parallel inverse Brayton cycle, which can be combined with Rankine cycle through using two heat exchangers as heat reservoir. The first law analysis and optimization for the
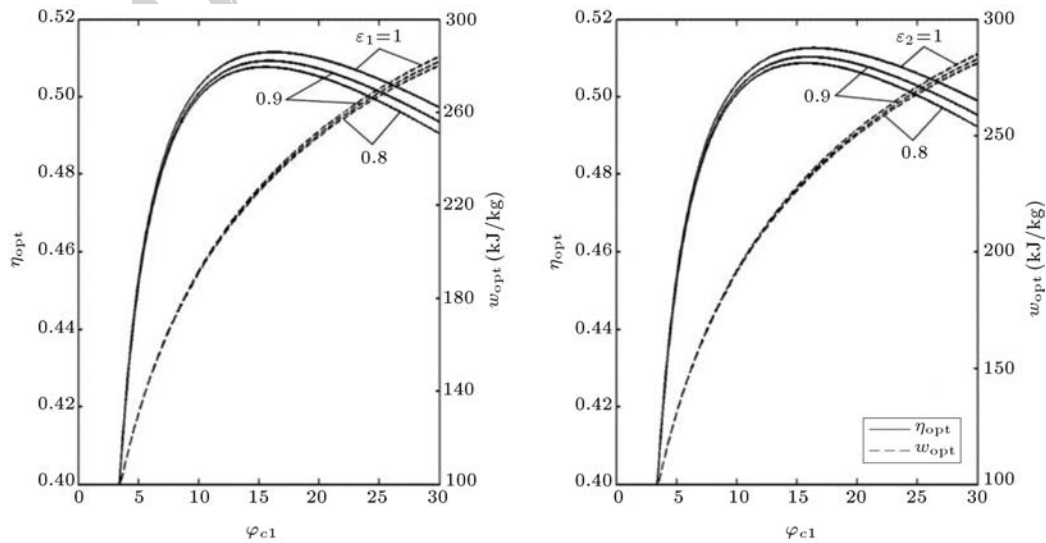

Figure 5: Influences of ε_1 and ε_2 on the η_{opt}–φ_{c1} and w_{opt}–φ_{c1} characteristics.
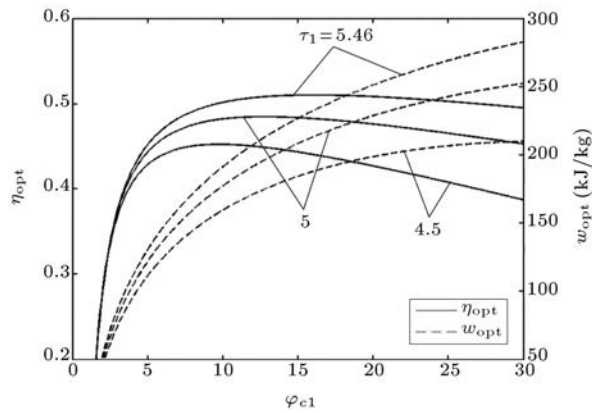
Figure 6: Influence of τ_1 on the η_{opt} –φ_{c1} and w_{opt} –φ_{c1} characteristics.

proposed combined cycle will be carried out by adjusting the compressor pressure ratios of the bottom cycles. Moreover, the influences of effectiveness of the regenerator and other parameters on the performance of the combined cycle will be analyzed by numerical examples.

2. Material and methods

The proposed combined cycle system layout is shown in Figure 1. It is constructed of a top regenerative Brayton cycle and two parallel bottom inverse Brayton cycles. The combined cycle recovers a part of heat energy before the working fluid entering the turbines of the inverse Brayton cycles as suggested in [10]. The top cycle is used as a gas generator to power the bottom cycles. The purpose of the turbine in the top cycle is solely to power the compressor in the top cycle. The power output of the combined cycle is totally produced by the two parallel bottom inverse cycles.

Figure 2 shows T–s diagram of the combined cycle. Process 1–2 is an irreversible adiabatic compression process in the compressor 1. Process 2–3 is an absorbed heat process in the regenerator. Process 3–4 is an absorbed heat process in the chamber. Process 4–5 is an irreversible adiabatic expansion process in the turbine 1. Process 5–6 is an evolved heat process

in the regenerator. Process 6–7 is an irreversible adiabatic expansion process in the turbine 2. Process 7–8 is an evolved heat process in the heat exchanger 1. Process 8–9 is an irreversible adiabatic compression process in the compressor 2. Process 6–10 is an irreversible adiabatic expansion process in the turbine 3. Process 10–11 is an evolved heat process in the heat exchanger 2. Process 11–12 is an irreversible adiabatic compression process in the compressor 3.

The following assumptions are made for simplicity and manipulating analytical expressions: The working fluid has constant specific heat ratio k ($k = c_P/c_V = 1.4$). The value of the mass flow rate $\dot{m}$ is fixed as 1 kg/s. The mass flow rate ratio λ ($0 \le \lambda \le 1$) is defined, which is the ratio of the mass flow rate of the first inverse Brayton cycle to the whole mass flow rate of the combined cycle.

The specific work required for compressor 1 of the regenerative Brayton cycle is:

$$w_{c1} = h_2 - h_1 = c_p T_1 \psi_{c1}/\eta_{c1}, \qquad (1)$$

where $\psi_{c1} = \varphi_{c1}^m - 1$, $m = (k-1)/k$, P is pressure, $\varphi_{c1} = P_2/P_1$ is pressure ratio of compressor 1, c_p is constant pressure specific heat, h is enthalpy and T is temperature.

The specific work output of turbine 1 of the regenerative Brayton cycle is:

$$w_{t1} = h_4 - h_5 = c_p T_1 \tau_1 \psi_{t1} \eta_{t1}, \qquad (2)$$

where $\psi_{t1} = 1 - 1/\varphi_{t1}^m$ and $\varphi_{t1} = P_4/P_5$ is pressure ratio of turbine 1, and $\tau_1 = T_4/T_1$ is temperature ratio of turbine 1.

The amount of heat added to the system in the combustion chamber is:

$$q_{in} = h_4 - h_3 = c_p T_1 \big[\tau_1 - \varepsilon_R \tau_1 (1 - \eta_{t1} \psi_{t1})$$
$$- (1 - \varepsilon_R)(\psi_{c1} + \eta_{c1})/\eta_{c1} \big], \qquad (3)$$

where ε_R is effectiveness of regenerator, η_{t1} and η_{c1} are internal efficiencies of turbine 1 and compressor 1, respectively.

The specific work output of turbine 2 of the first inverse Brayton cycle is:

$$w_{t2} = h_5 - h_6 = \lambda c_p T_1 \eta_{t2} \psi_{t2} (\tau_1 - \psi_{c1}/\eta_{c1}), \qquad (4)$$

where $\psi_{t2} = 1 - 1/\varphi_{t2}^m$ and $\varphi_{t2} = P_5/P_6$ is pressure ratio of turbine 2 and η_{t2} is internal efficiency of turbine 2.
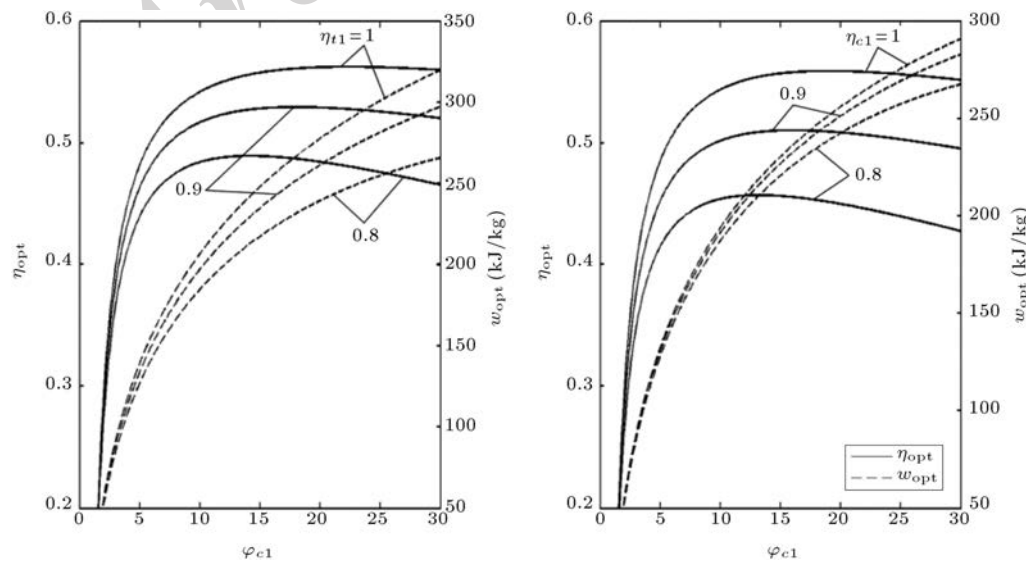

Figure 7: Influences of η_{t1}, η_{c1} on the η_{opt} –φ_{c1} and w_{opt} –φ_{c1} characteristics.
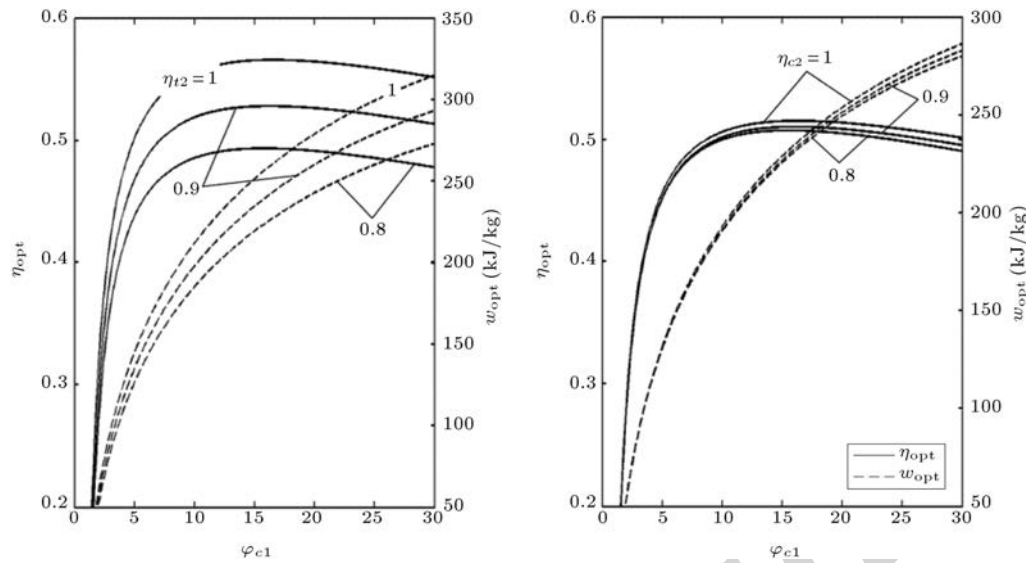
Figure 8: Influences of η_{t2}, η_{c2} on the η_{opt} –φ_{c1} and w_{opt} –φ_{c1} characteristics.
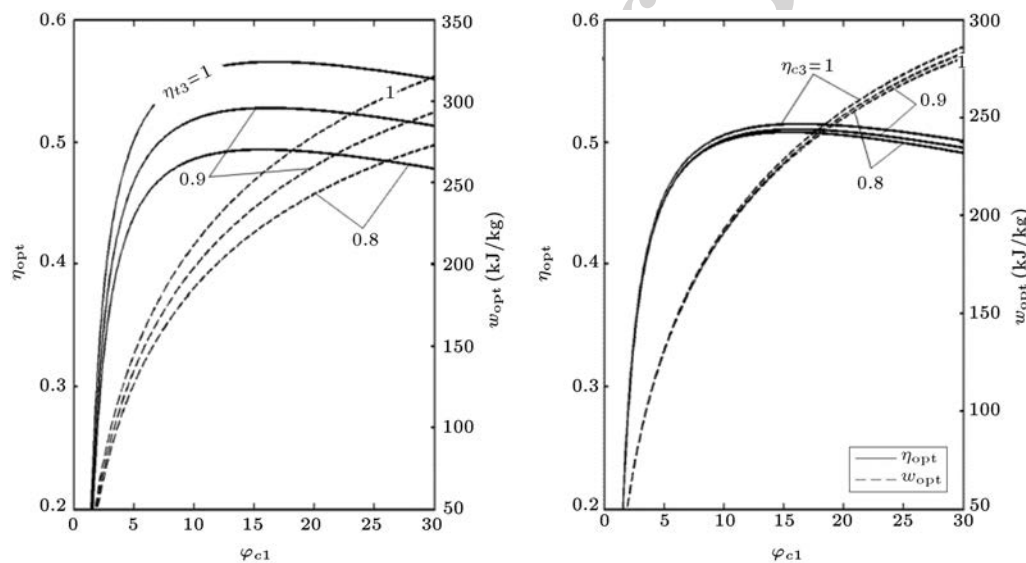

Figure 9: Influences of η_{t3}, η_{c3} on the η_{opt} –φ_{c1} and w_{opt} –φ_{c1} characteristics.

The specific work required for compressor 2 of the first inverse Brayton cycle is:

$$w_{c2} = h_9 - h_8$$
$$= \lambda c_p T_1 \{(1 - \eta_{t2}\psi_{t2})(1 - \varepsilon_1)[\varepsilon_R(\psi_{c1} + \eta_{c1})/\eta_{c1}$$
$$+ \tau_1(1 - \varepsilon_R)(1 - \eta_{t1}\psi_{t1})] + \varepsilon_1\}\psi_{c2}/\eta_{c2} \qquad (5)$$

where $\psi_{c2} = \varphi_{c2}^m - 1$ and $\varphi_{c2} = P_9/P_8$ is pressure ratio of compressor 2, η_{c2} is internal efficiency of compressor 2 and ε_1 is effectiveness of heat exchanger 1.

The specific work output of turbine 3 of the second inverse Brayton cycle is:

$$w_{t3} = h_6 - h_{10} = (1 - \lambda) c_p T_1 \eta_{t2}\psi_{t2}[\varepsilon_R(\psi_{c1} + \eta_{c1})/\eta_{c1}$$
$$+ \tau_1(1 - \varepsilon_R)(1 - \eta_{t3}\psi_{t3})], \qquad (6)$$

where $\psi_{t3} = 1 - 1/\varphi_{t3}^m$ and $\varphi_{t3} = P_6/P_{10}$ is pressure ratio of turbine 3, η_{t3} is internal efficiency of turbine 3.

The specific work required for compressor 3 of the second inverse Brayton cycle is:

$$w_{c3} = h_{12} - h_{11}$$
$$= (1 - \lambda) c_p T_1 \{(1 - \eta_{t3}\psi_{t3})(1 - \varepsilon_2)$$
$$\times [\varepsilon_R(\psi_{c1} + \eta_{c1})/\eta_{c1} + \tau_1(1 - \varepsilon_R)$$
$$\times (1 - \eta_{t1}\psi_{t1})] + \varepsilon_2\}\psi_{c3}/\eta_{c3}, \qquad (7)$$

where $\psi_{c3} = \varphi_{c3}^m - 1$ and $\varphi_{c3} = P_{12}/P_{11}$ is pressure ratio of compressor 3, η_{c3} is internal efficiency of compressor 3 and ε_2 is effectiveness of heat exchanger 2.

For turbine 1 is solely used to power the compressor 1 ($w_{c1} = w_{t1}$), one can derive the following expression:

$$\varphi_{t1} = [\eta_{c1}\eta_{t1}\tau_1/(\eta_{c1}\eta_{t1}\tau_1 - \varphi_{c1}^m + 1)]^{\frac{1}{m}}. \qquad (8)$$
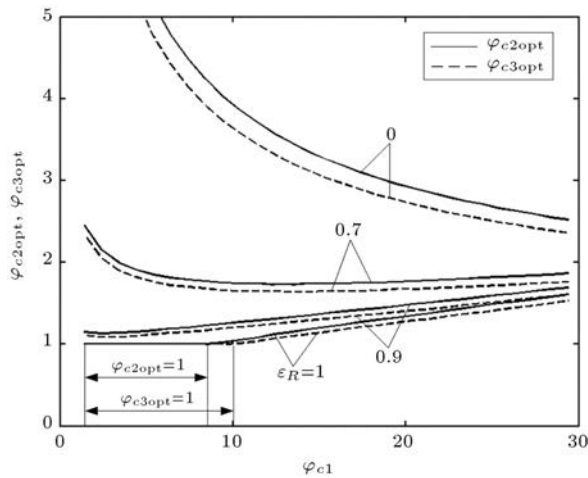
Figure 10: Influence of ε_R on the φ_{c2opt} –φ_{c1} and φ_{c3opt} –φ_{c1} characteristics.

For the total ratios of expansion and compression are equal ($\varphi_{t2} = D_1\varphi_{c1}\varphi_{c2}/\varphi_{t1}$, $\varphi_{t3} = D_2\varphi_{c1}\varphi_{c3}/\varphi_{t1}$), one can derive the following expressions:

$$\psi_{t2} = 1 - \frac{\eta_{c1}\eta_{t1}\tau_1}{D_1^m(\psi_{c1}+1)(\eta_{c1}\eta_{t1}\tau_1-\psi_{c1})\varphi_{c2}^m}, \qquad (9)$$

$$\psi_{t3} = 1 - \frac{\eta_{c1}\eta_{t1}\tau_1}{D_2^m(\psi_{c1}+1)(\eta_{c1}\eta_{t1}\tau_1-\psi_{c1})\varphi_{c3}^m}, \qquad (10)$$

where $D_1 = P_1/P_9$ and $D_2 = P_1/P_{12}$.

The specific work outputs of the first inverse and the second inverse Brayton cycle are:

$$\begin{aligned}
w_{g1} &= w_{t2} - w_{c2} \\
&= \lambda c_p T_1 \eta_{t2}\left(1 - a/\varphi_{c2}^m\right)\left[\varepsilon_R c + b\left(1-\varepsilon_R\right)\right] \\
&\quad - \lambda c_p T_1\big\{\left[1 - \eta_{t2}\left(1 - a/\varphi_{c2}^m\right)\right]\left[\varepsilon_R c + b\left(1-\varepsilon_R\right)\right] \\
&\quad \times \left(1-\varepsilon_1\right) + \varepsilon_1\big\}(\varphi_{c2}^m-1)/\eta_{c2}, \qquad (11)
\end{aligned}$$

$$\begin{aligned}
w_{g2} &= w_{t3} - w_{c3} = (1-\lambda)\,c_p T_1 \eta_{t3}\left(1 - d/\varphi_{c3}^m\right) \\
&\quad \times \left[\varepsilon_R c + b\left(1-\varepsilon_R\right)\right] - (1-\lambda)\,c_p T_1 \\
&\quad \times \big\{\left[1 - \eta_{t3}\left(1 - d/\varphi_{c3}^m\right)\right]\left[\varepsilon_R c + b\left(1-\varepsilon_R\right)\right] \\
&\quad \times \left(1-\varepsilon_2\right) + \varepsilon_2\big\}(\varphi_{c3}^m - 1)/\eta_{c3} \qquad (12)
\end{aligned}$$

where:

$a = \eta_{c1}\eta_{t1}\tau_1/[D_1^m(\psi_{c1}+1)(\eta_{c1}\eta_{t1}\tau_1 - \psi_{c1})]$,

$b = \tau_1(1 - \eta_{t1}\psi_{t1})$,

$c = 1 + \psi_{c1}/\eta_{c1}$ and

$d = \eta_{c1}\eta_{t1}\tau_1/[D_2^m(\psi_{c1}+1)(\eta_{c1}\eta_{t1}\tau_1 - \psi_{c1})]$.

The specific work output and the thermal efficiency of the whole system are: Eqs. (13) and (14) are given in Box I.

Combining Eq. (13) with Eq. (14), one can find that for the first inverse Brayton cycle the extremal conditions of $\partial\eta/\partial\varphi_{c2} = 0$ and $\partial w/\partial\varphi_{c2} = 0$ are the same, and for the second inverse Brayton cycle, the external conditions of $\partial\eta/\partial\varphi_{c3} = 0$ and $\partial w/\partial\varphi_{c3} = 0$ are also the same. Thus, the optimal pressure ratios of compressor 2 and compressor 3 corresponding to the maximum specific work output and the maximum thermal efficiency are: Eqs. (15) and (16) are given in Box II respectively.

When the parameters of the first inverse Brayton cycles are the same as the second inverse Brayton cycle, the performance of the combined cycle is also the same as the combined regenerative Brayton and inverse Brayton cycles proposed in [10]. In order to meet the practical applications, the mass flow rate ratio can be adjusted under different conditions.

3. Result and discussions

To see how various parameters influence the thermal efficiency and specific work of the combined cycle, numerical examples are provided. In the calculations, it is set that $\lambda = 0.5$, $\eta_{c1} = \eta_{c2} = \eta_{c3} = 0.9$, $\eta_{t1} = \eta_{t2} = \eta_{t3} = 0.85$, $T_1 = 288.15$ K, $P_1 = 0.1013$ MPa, $P_9 = P_{12} = 0.104$ MPa, $\varepsilon_1 = 0.95$, $\varepsilon_2 = 0.9$ and $\varepsilon_R = 0.9$. If the parameters of the two parallel bottom cycles are the same, λ has no influence on the performance of the combined cycles.

Figures 3–9 show the influences of the effectiveness (ε_R) of the regenerator, the mass flow rate ratio (λ), the effectiveness
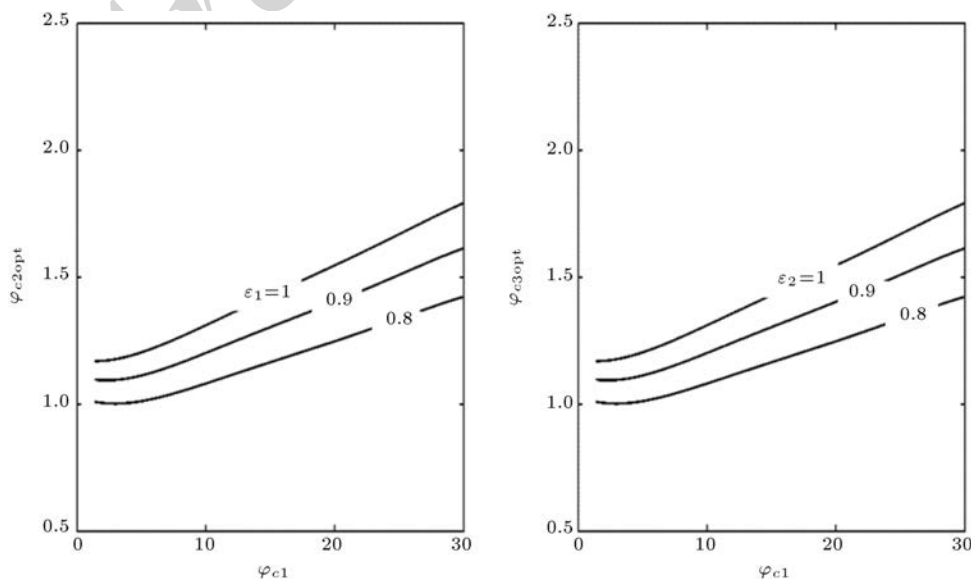

Figure 11: Influences of ε_1, ε_2 on the φ_{c2opt} –φ_{c1} and φ_{c3opt} –φ_{c1} characteristics.

$$
\begin{aligned}
w &= w_{g1} + w_{g2} = \lambda c_p T_1 \eta_{t2}(1 - a/\varphi_{c2}^m)\,[\varepsilon_R c + b(1 - \varepsilon_R)] - [\lambda c_p T_1(\varphi_{c2}^m - 1)/\eta_{c2}] \times \{[1 - \eta_{t2}(1 - a/\varphi_{c2}^m)] \\
&\quad \times [\varepsilon_R c + b(1 - \varepsilon_R)](1 - \varepsilon_1) + \varepsilon_1\} + (1 - \lambda)c_p T_1 \eta_{t3}(1 - d/\varphi_{c3}^m)\,[\varepsilon_R c + b(1 - \varepsilon_R)] - [(1 - \lambda)c_p T_1(\varphi_{c3}^m - 1)/\eta_{c3}] \\
&\quad \times \{[1 - \eta_{t3}(1 - d/\varphi_{c3}^m)][\varepsilon_R c + b(1 - \varepsilon_R)](1 - \varepsilon_2) + \varepsilon_2\}
\end{aligned}
\tag{13}
$$

$$
\begin{aligned}
\eta &= w/q_{in} \\
&= \cfrac{\begin{aligned}&\lambda \eta_{t2}(1 - a/\varphi_{c2}^m)\,[\varepsilon_R c + b(1 - \varepsilon_R)] - [\lambda(\varphi_{c2}^m - 1)/\eta_{c2}] \times \{[1 - \eta_{t2}(1 - a/\varphi_{c2}^m)][\varepsilon_R c + b(1 - \varepsilon_R)](1 - \varepsilon_1) + \varepsilon_1\} \\ &+ (1 - \lambda)\eta_{t3}(1 - d/\varphi_{c3}^m)\,[\varepsilon_R c + b(1 - \varepsilon_R)] - [(1 - \lambda)(\varphi_{c3}^m - 1)/\eta_{c3}] \\ &\times \{[1 - \eta_{t3}(1 - d/\varphi_{c3}^m)][\varepsilon_R c + b(1 - \varepsilon_R)](1 - \varepsilon_2) + \varepsilon_2\}\end{aligned}}{\tau_1 - \varepsilon_R b - (1 - \varepsilon_R)c}
\end{aligned}
\tag{14}
$$

Box I

$$
\varphi_{c2opt} = \left\{ \frac{a[b(\varepsilon_R - 1) - c\varepsilon_R](\varepsilon_1 - 1 + \eta_{c2})\eta_{t2}}{b(\varepsilon_R - 1)(\varepsilon_1 - 1)(\eta_{t2} - 1) + c\varepsilon_R(\eta_{t2} - 1) + \varepsilon_1(c\varepsilon_R - c\varepsilon_R\eta_{t2} - 1)} \right\}^{1/m},
\tag{15}
$$

$$
\varphi_{c3opt} = \left\{ \frac{d[b(\varepsilon_R - 1) - c\varepsilon_R](\varepsilon_2 - 1 + \eta_{c3})\eta_{t3}}{b(\varepsilon_R - 1)(\varepsilon_2 - 1)(\eta_{t3} - 1) + c\varepsilon_R(\eta_{t3} - 1) + \varepsilon_2(c\varepsilon_R - c\varepsilon_R\eta_{t3} - 1)} \right\}^{1/m}
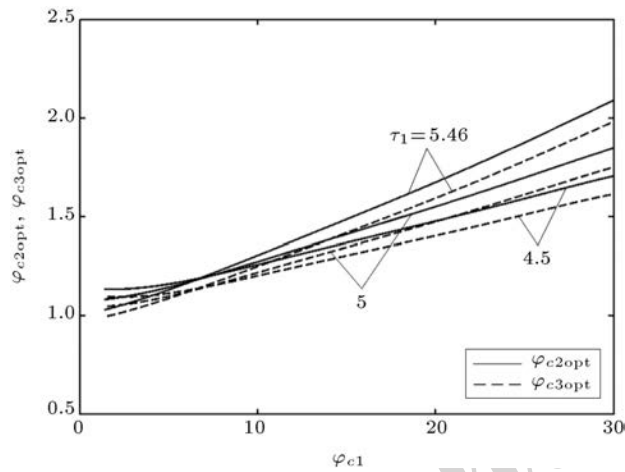\tag{16}
$$

Box II

Figure 12: Influence of τ_1 on the φ_{c2opt}–φ_{c1} and φ_{c3opt}–φ_{c1} characteristics.

(ε_1) of the heat exchanger 1, the effectiveness (ε_2) of the heat exchanger 2, the temperature ratio (τ_1), the compressor internal efficiencies η_{c1}, η_{c2} and η_{c3} as well as the turbine internal efficiencies η_{t1}, η_{t2} and η_{t3} on the η_{opt}–φ_{c1} and w_{opt}–φ_{c1} characteristics, respectively. From Figure 3, one can see that η_{opt} increases with an increase in ε_R, and there exists an optimal pressure ratio (φ_{c1opt}) of compressor 1 which leads to the maximum optimal thermal efficiency ($\eta_{opt\,max}$) when ε_R is high enough. In the critical range of φ_{c1}, the optimal thermal efficiency (η_{opt}) of the regenerative combined cycle ($\varepsilon_R > 0$) is always larger than that of the simple combined cycle ($\varepsilon_R = 0$). w_{opt} decreases with an increase in ε_R; w_{opt} increases with an increase in φ_{c1} when $\varepsilon_R > 0$; there exists an optimal pressure ratio of compressor 1 which leads to the maximum optimal specific work ($w_{opt\,max}$) when $\varepsilon_R = 0$. The optimal specific work (w_{opt}) of the regenerative combined cycle ($\varepsilon_R > 0$) is always smaller than that of the simple combined cycle ($\varepsilon_R = 0$). From Figures 4–9, one can see that both η_{opt} and w_{opt} increase with the increases in λ, ε_1, ε_2, τ_1, η_{c1}, η_{t1}, η_{c2}, η_{t2}, η_{c3} and η_{t3}.

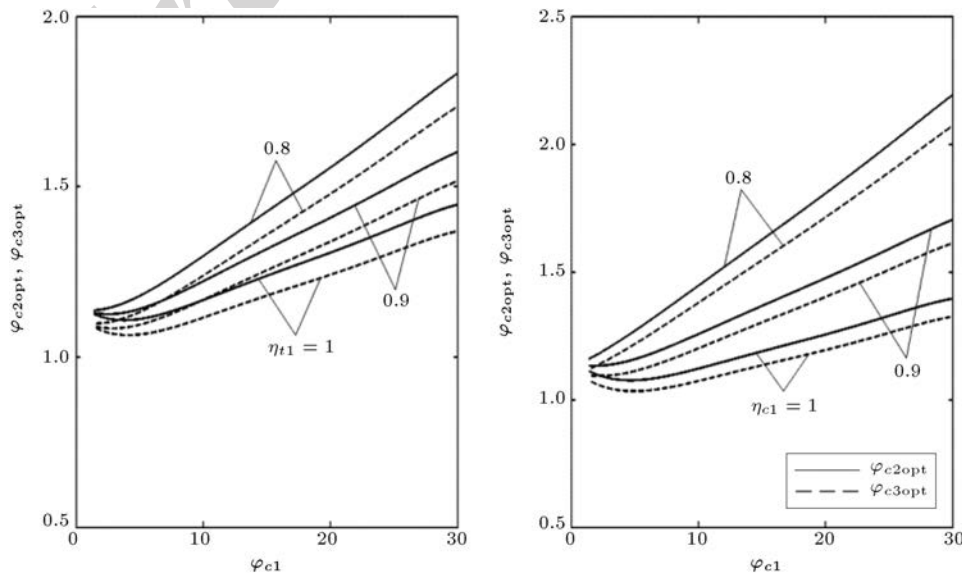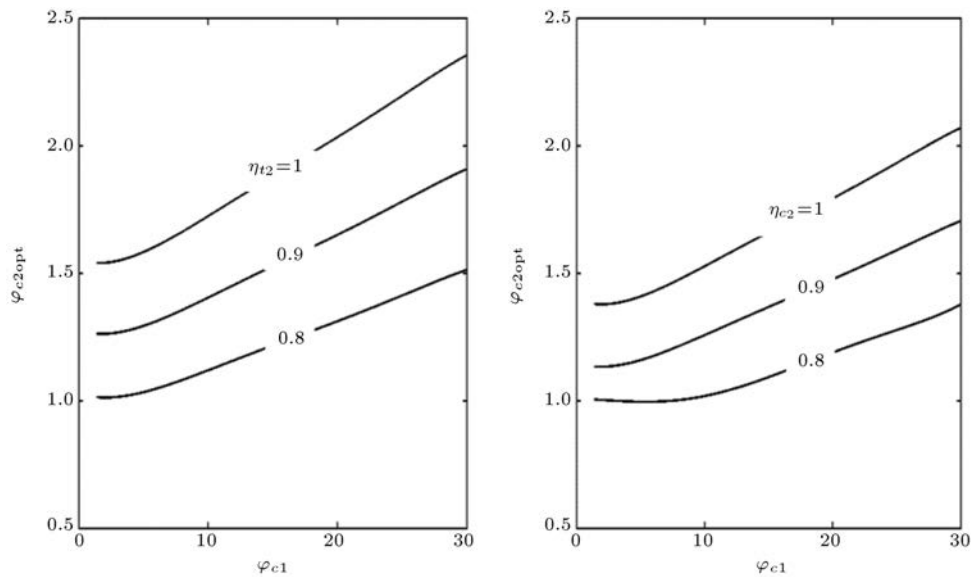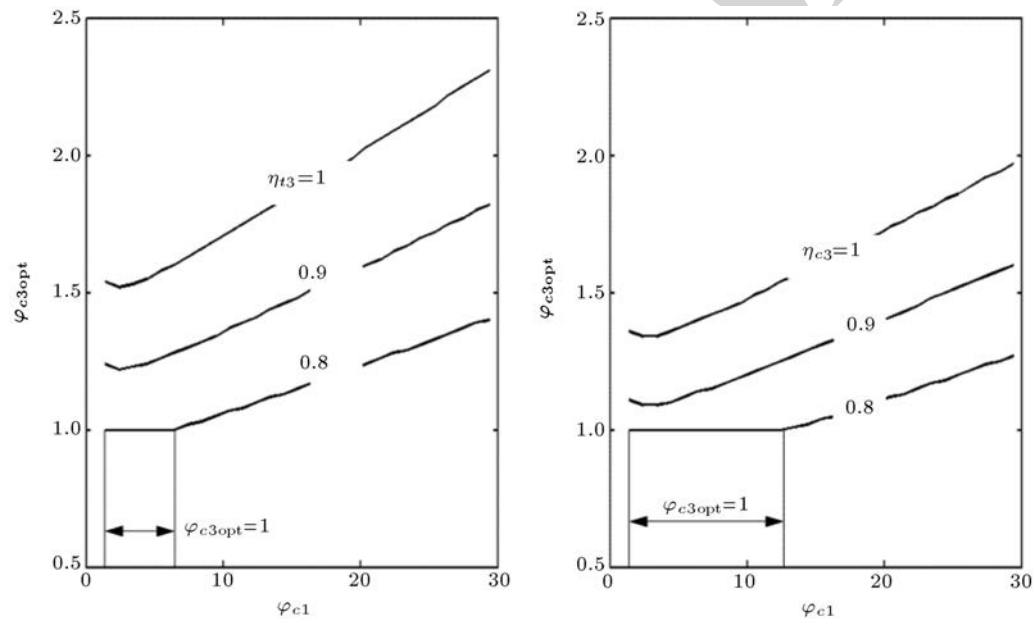Figure 13: Influences of η_{t1}, η_{c1} on the φ_{c2opt}–φ_{c1} and φ_{c3opt}–φ_{c1} characteristics.

Figure 14: Influences of η_{t2}, η_{c2} on the φ_{c2opt} –φ_{c1} and φ_{c3opt} –φ_{c1} characteristics.

Figure 15: Influences of η_{t3}, η_{c3} on the φ_{c2opt} –φ_{c1} and φ_{c3opt} –φ_{c1} characteristics.

Figures 10–15 show the influences of the effectiveness (ε_R) of the regenerator, the effectiveness (ε_1) of the heat exchanger 1, the effectiveness (ε_2) of the heat exchanger 2, the temperature ratio (τ_1), the compressor internal efficiencies η_{c1}, η_{c2} and η_{c3} as well as the turbine internal efficiencies η_{t1}, η_{t2} and η_{t3} on the φ_{c2opt} –φ_{c1} and φ_{c3opt} –φ_{c1} characteristics, respectively. From Figure 10, one can see that both the optimal pressure ratio (φ_{c2opt}) of the compressor 2 and the optimal pressure ratio (φ_{c3opt}) of the compressor 3 decrease with the increase in ε_R. In the critical range of φ_{c1} shown in Figure 10, the values of φ_{c2opt} and φ_{c3opt} will equal to 1 when $\varepsilon_R = 1$. In other words, the compressor 2 and the compressor 3 should be canceled under these conditions. From Figures 11–15, one can see that both φ_{c2opt} and φ_{c3opt} increase with the increases in φ_{c1}, ε_1, ε_2, τ_1, η_{c2}, η_{c3} and η_{t3}, whereas they decrease with the increases in η_{c1} and η_{t1}.

4. Conclusion

A configuration of combined regenerative Brayton and two parallel inverse Brayton cycles with regeneration before the inverse cycles is established in this paper. The combined cycle proposed herein recovers a part of heat energy contained in the exhaust gases leaving the turbine of the top cycle. This paper provides a clear idea about the performance of the combined regenerative cycle by taking the first law analysis and optimization. The thermal efficiency and the specific work are optimized by adjusting the compressor pressure ratios of the bottom cycles. The influences of effectiveness of the regenerator and other parameters on the optimal thermal efficiency and optimal specific work are analyzed. It is found that the combined regenerative cycle can obtain higher thermal efficiency than that of the base cycle but with smaller work

output, and the performance of the combined cycle (with two parallel inverse Brayton cycles) proposed in this paper is the same as the combined cycle (with one inverse Brayton cycle) proposed in [10] when the parameters of the two inverse Brayton cycles are the same. One can adjust the mass flow ratio and other parameters of the combined cycle in different practical applications. Further steps will be the second law analysis and optimization and finite time thermodynamic optimization for the proposed cycle.

Acknowledgments

References

[1] Frutschi, H.U. and Plancherel, A.A. "Comparison of combined cycles with steam injection and evaporation cycles", *Proc. ASME COGEN-TURBO II*, pp. 137–145 (1988).

[2] Vecchiarelli, J., Kawall, J.G. and Wallace, J.S. "Analysis of a concept for increasing the efficiency of a Brayton cycle via isothermal heat addition", *Int. J. Energy Res.*, 21(2), pp. 113–127 (1997).

[3] Horlock, J.D., *Advanced Gas Turbine Cycles*, Elsevier Science, Oxford (2003).

[4] Sato, H., *Cycle Theory of Gas Turbine*, Sankaido, Tokyo (1972).

[5] Chase, D.L. "Combined cycle development evolution and future", GER-4206, GE Power Systems (2001).

[6] Frost, T.H., Anderson, A. and Agnew, B. "A hybrid gas turbine cycle (Brayton/Ericsson): an alternative to conventional combined gas and steam turbine power plant", *Proc. Inst. Mech. Eng. Part A*, 211(A2), pp. 121–131 (1997).

[7] Fujii, S., Kaneko, K. and Tsujikawa, K. "Mirror gas turbine: a newly proposed method of exhaust heat recovery", *Trans. ASME, J. Eng. Gas Turbines Power*, 123(2), pp. 481–486 (2001).

[8] Bianchi, M., Negri di Montenegro, G. and Peretto, A. "Inverted Brayton cycle employment for low temperature cogeneration applications", *Trans. ASME, J. Eng. Gas Turbines Power*, 124(2), pp. 561–565 (2002).

[9] Agnew, B., Anderson, A., Potts, I., Frost, T.H. and Alabdoadaim, M.A. "Simulation of combined Brayton and inverse Brayton cycles", *Appl. Therm. Eng.*, 23(8), pp. 953–963 (2003).

[10] Alabdoadaim, M.A., Agnew, B. and Potts, I. "Performance analysis of combined Brayton and inverse Brayton cycles and developed configurations", *Appl. Therm. Eng.*, 26(14–15), pp. 1448–1454 (2006).

[11] Alabdoadaim, M.A., Agnew, B. and Alaktiwi, A. "Examination of the performance envelope of combined Rankine, Brayton and two parallel inverse Brayton cycles", *Proc. Inst. Mech. Eng. Part A*, 218(6), pp. 377–385 (2004).

[12] Alabdoadaim, M.A., Agnew, B. and Potts, I. "Examination of the performance of an unconventional combination of Rankine, Brayton and inverse Brayton cycles", *Proc. Inst. Mech. Eng. Part A*, 220(4), pp. 305–313 (2006).

[13] Zheng, J.L., Sun, F.R., Chen, L.G. and Wu, C. "Exergy analysis for a Braysson cycle", *Int. J. Exergy*, 1(1), pp. 41–45 (2001).

[14] Zhang, W.L., Chen, L.G., Sun, F.R. and Wu, C. "Second-law analysis and optimization for combined Brayton and inverse Brayton cycles", *Int. J. Ambient Energy*, 28(1), pp. 15–26 (2007).

[15] Zhang, W.L., Chen, L.G., Sun, F.R. and Wu, C. "Second law analysis and parametric study for combined Brayton and two parallel inverse Brayton cycles", *Int. J. Ambient Energy*, 30(4), pp. 179–192 (2009).

[16] Zheng, J.L., Chen, L.G., Sun, F.R. and Wu, C. "Power and efficiency performance of an endoreversible Braysson cycle", *Int. J. Thermal Sci.*, 41(2), pp. 201–205 (2002).

[17] Zheng, T., Chen, L.G., Sun, F.R. and Wu, C. "Power, power density and efficiency optimization of an endoreversible Braysson cycle", *Int. J. Exergy*, 2(4), pp. 380–386 (2002).

[18] Zhang, W.L., Chen, L.G. and Sun, F.R. "Power and efficiency optimization for combined Brayton and inverse Brayton cycles", *Appl. Therm. Eng.*, 29(14–15), pp. 2885–2894 (2009).

[19] Chen, L.G., Zhang, W.L. and Sun, F.R. "Power and efficiency optimization for combined Brayton and two parallel inverse Brayton cycles, Part 1: description and modeling", *Proc. Inst. Mech. Eng. Part C*, 222(C3), pp. 393–403 (2008).

[20] Zhang, W.L., Chen, L.G. and Sun, F.R. "Power and efficiency optimization for combined Brayton and two parallel inverse Brayton cycles. Part 2: performance optimization", *Proc. Inst. Mech. Eng. Part C*, 222(C3), pp. 405–414 (2008).

[21] Andresen, B., Salamon, P. and Berry, R.S. "Thermodynamics in finite time", *Phys. Today*, pp. 62–70 (1984).

[22] Sieniutycz, S. and Salamon, P., *"Finite time thermodynamics and thermoeconomics"*, In *Advances in Thermodynamics*, 4, Taylor & Francis, New York (1990).

[23] Bejan, A. "Entropy generation minimization: the new thermodynamics of finite-size devices and finite-time processes", *J. Appl. Phys.*, 79(3), pp. 1191–1218 (1996).

[24] Feidt, M. "Optimization of Brayton cycle engine in contact with fluid thermal capacities", *Rev. Gen. Therm.*, 35(418–419), pp. 662–666 (1996).

[25] Chen, L.G., Wu, C. and Sun, F.R. "Finite time thermodynamic optimization or entropy generation minimization of energy systems", *J. Non-Equilib. Thermodyn.*, 24(4), pp. 327–359 (1999).

[26] Salamon, P., Nulton, J.D., Siragusa, G., Andresen, T.R. and Limon, A. "Principles of control thermodynamics", *Energy Int. J.*, 26(3), pp. 307–319 (2001).

[27] Bejan, A. "Fundamentals of exergy analysis, entropy generation minimization, and the generation of flow architecture", *Int. J. Energy Res.*, 26(7), pp. 545–565 (2002).

[28] Chen, L.G., *Finite-Time Thermodynamic Analysis of Irreversible Processes and Cycles*, Higher Education Press, Beijing (2005).

[29] Feidt, M., Costea, M. and Postelnicu, V. "Comparison between the Brayton cycle with imposed thermal input and with maximum temperature constraint", *Oil Gas Sci. Tech.*, 61(2), pp. 237–245 (2006).

[30] Sieniutycz, S. and Jezowski, J., *Energy Optimization in Process Systems*, Elsevier, Oxford, UK (2009).

[31] Feidt, M. "Optimal thermodynamics—New upperbounds", *Entropy*, 11(4), pp. 529–547 (2009).

[32] Andresen, B. "Current trends in finite-time thermodynamics", *Angew. Chem. Int. Ed.*, 50(12), pp. 2690–2704 (2011).

[33] Costea, M., Feidt, M., Alexandru, G. and Descieux, D. "Optimization of gas turbine cogeneration system for various heat exchanger configurations", *Oil Gas Sci. Tech.* (in press).

Zelong Zhang received his B.S. Degree in 2009 in heat energy and power engineering from the Huazhong University of Science and Technology, M.S. Degree in 2011 in power engineering and engineering thermophysics of Naval University of Engineering, PR China. His work covers topics in finite time thermodynamics and technology support for propulsion plants. He is the author and co-author of 7 peer-refereed articles (4 in English journals).

Lingen Chen received all his degrees (B.S., 1983; M.S., 1986; Ph.D., 1998) in power engineering and engineering thermophysics from the Naval University of Engineering, PR China. His work covers a diversity of topics in engineering thermodynamics, constructal theory, turbomachinery, reliability engineering, and technology support for propulsion plants. He was the Director of the Department of Nuclear Energy Science and Engineering, the Director of the Department of Power Engineering and the Superintendent of the Postgraduate School. Now, he is President of the College of Naval Architecture and Power, Naval University of Engineering, PR China. Professor Chen is the author and co-author of over 1220 peer-refereed articles (over 560 in English journals) and nine books (two in English).

Fengrui Sun received his B.S. degree in 1958 in Power Engineering from the Harbing University of Technology, PR China. His work covers a diversity of topics in engineering thermodynamics, constructal theory, reliability engineering, and marine nuclear reactor engineering. He is a Professor in the Department of Power Engineering, Naval University of Engineering, PR China. Professor Sun is the author and co-author of over 950 peer-refereed papers (over 440 in English) and two books (one in English).